TrkB hyperactivity contributes to brain dysconnectivity, epileptogenesis, and anxiety in a zebrafish model of Tuberous Sclerosis Complex

Magdalena Kedra[1], Katarzyna Banasiak[1], Katarzyna Kisielewska[1], Lidia Wolinska-Niziol[1], Jacek Jaworski[1]*, Justyna Zmorzynska[1]*

[1]Laboratory of Molecular and Cellular Neurobiology, International Institute of Molecular and Cell Biology in Warsaw

Supplemental Information

www.pnas.org/cgi/doi/10.1073/pnas.1910834117

Supplementary Figures

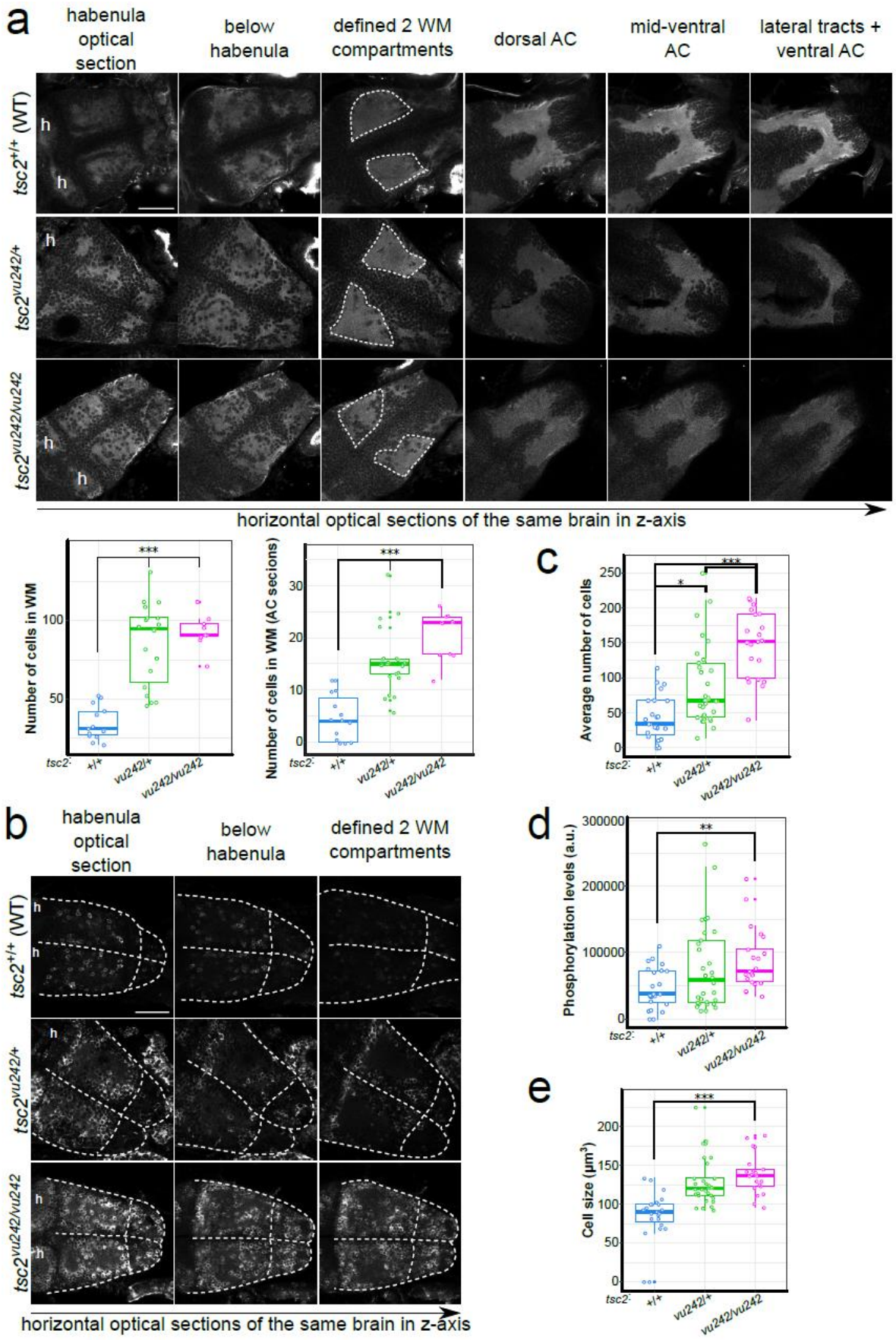
a
habenula optical section
below habenula
defined 2 WM compartments
dorsal AC
mid-ventral AC
lateral tracts + ventral AC
tsc2+/+ (WT)
tsc2vu242/+
tsc2vu242/vu242
h
horizontal optical sections of the same brain in z-axis
Number of cells in WM
Number of cells in WM (AC secions)
tsc2-: +/+ vu242/+ vu242/vu242
***
b
habenula optical section
below habenula
defined 2 WM compartments
horizontal optical sections of the same brain in z-axis
c
Average number of cells
*
***
d
Phosphorylation levels (a.u.)
**
e
Cell size (μm3)

Fig. S1. a, Photomicrographs of horizontal optical sections of the *tsc2*^{vu242} zebrafish brain that were immunostained with anti-acetylated Tubulin (ac-Tubulin) antibody. Defined white matter (WM) compartments are framed with a dashed line. h, habenula; AC, anterior commissure. Scale bar = 40 μm. Box-plots fo the 3D quantification show total number of cells in the WM compartments ($F = 32.95$, $p = 6.0 \times 10^{-9}$; $p < 0.0001$ for *tsc2*$^{vu242/vu242}$ and *tsc2*$^{vu242/+}$ *vs*. *tsc2*$^{+/+}$ [Dunnett's test]) and the number of cells in WM compartments on the z-level of the AC ($H = 27.917$, $p = 8.67 \times 10^{-7}$; $p < 0.0001$ for *tsc2*$^{vu242/vu242}$ and *tsc2*$^{vu242/+}$ *vs. tsc2*$^{+/+}$ [Dunn's test]). **b**, Photomicrographs of horizontal optical sections of the *tsc2*^{vu242} zebrafish brain that were immunostained with anti-P-Rps6 antibody. h, habenula. Scale bar = 40 μm. **c**, The number of P-Rps6-positive neurons in the telencephalon in *tsc2*^{vu242} fish from 3D analysis of the whole-brain confocal images ($H = 32.251$, $p = 9.925 \times 10^{-8}$; $p = 4.1 \times 10^{-8}$ for *tsc2*$^{vu242/vu242}$ *vs*. *tsc2*$^{+/+}$, $p = 0.0045$ for *tsc2*$^{vu242/vu242}$ *vs*. *tsc2*$^{vu242/+}$, $p = 0.0104$ for *tsc2*$^{vu242/+}$ *vs*. *tsc2*$^{+/+}$ [Dunn's test]). **d,** Phosphorylation levels of P-Rps6 per cell in the telencephalon in *tsc2*^{vu242} fish from 3D analysis of the whole-brain confocal images ($H = 8.8944$, $p = 0.0117$; $p = 0.0086$ for *tsc2*$^{vu242/vu242}$ *vs*. *tsc2*$^{+/+}$ [Dunnett's test]). **e,** Soma size of P-Rps6-positive neurons in the telencephalon in *tsc2*^{vu242} fish from 3D analysis of the whole-brain confocal images ($F = 20.71$, $p = 8.19 \times 10^{-8}$; $p = 2.34 \times 10^{-7}$ for *tsc2*$^{vu242/vu242}$ *vs*. *tsc2*$^{+/+}$ [Dunnett's test]). *$p < 0.05$, **$p < 0.01$, ***$p < 0.001$.

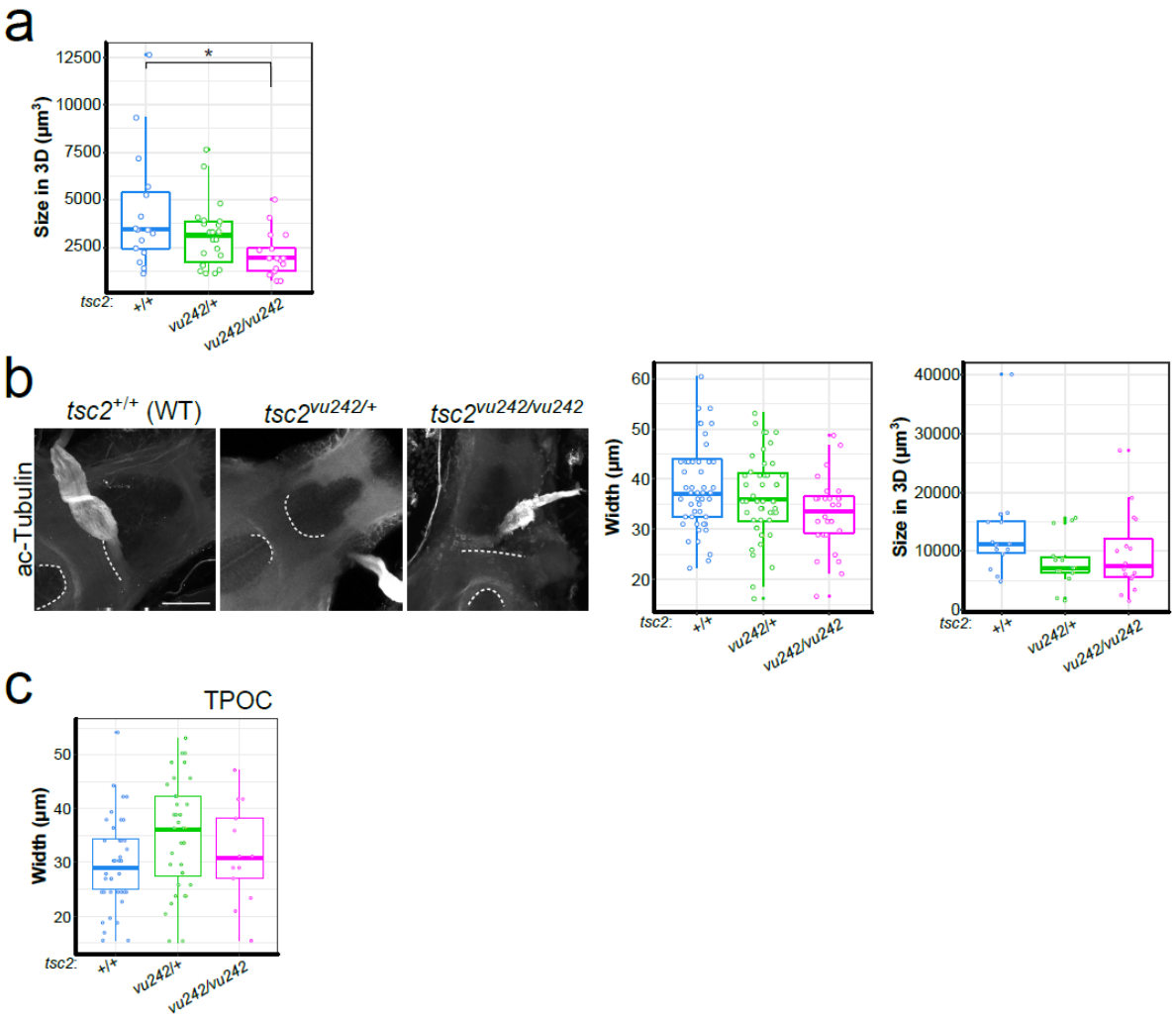

Fig. S2. a, Boxplot of the quantification of anterior commissure in 3D from whole-brain confocal imaging ($H = 8.884$, $p = 0.094$; $p = 0.011$ for *tsc2*$^{vu242/vu242}$ *vs.* *tsc2*$^{+/+}$ [Dunn's test]). **b**, Representative confocal horizontal optical sections of the *tsc2*^{vu242} zebrafish brain that were immunostained with anti-acetylated Tubulin (ac-Tubulin) antibody that show the postoptic commissure (POC; dashed lines) with quantification of POC width and volume that shows a decrease that corresponds to the mutation of the *tsc2* gene. Scale bar = 40 µm. **c**, Boxplots of the width of tracts of the POC in *tsc2*^{vu242} zebrafish. TPOC, tracts of postoptic commissure. *$p < 0.05$.

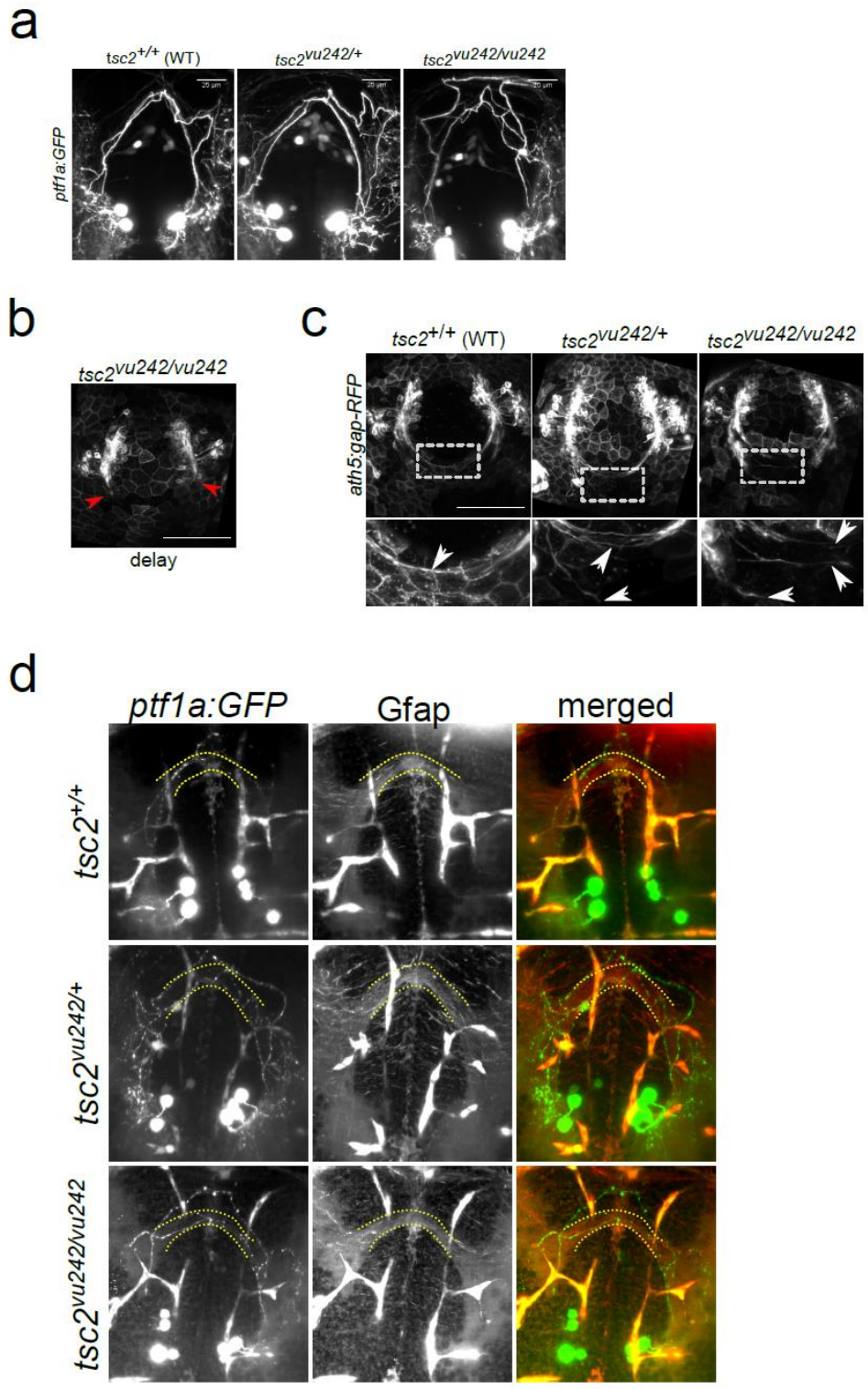

Fig. S3. **a**, Representative confocal images of a dorsal view of *ptf1a:GFP*-positive commissures in the brain in *tsc2*^{vu242} zebrafish that show severe phenotypes of axonal tract fasciculation. **b**, Frontal view of *ath5:gap-RFP*-positive neurons without elongated axons (red arrows) in the brains in *tsc2*$^{vu242/vu242}$ zebrafish that represent developmental delay. Scale bar =

100 μm. **c**, Representative confocal images of a frontal view of *ath5:gap-RFP*-positive axons in the brain in *tsc2*^{vu242} zebrafish that show defects in axon bundling and elongation toward the brain midline in *tsc2*$^{vu242/vu242}$ and *tsc2*$^{vu242/+}$ mutant fish at 27 hpf. Scale bar = 100 μm. **d**, Representative photomicrographs of dorsally acquired whole mounts of the *tsc2*^{vu242} zebrafish brain with *ptf1a:GFP*-positive commissures that were stained with anti-Gfap antibody.

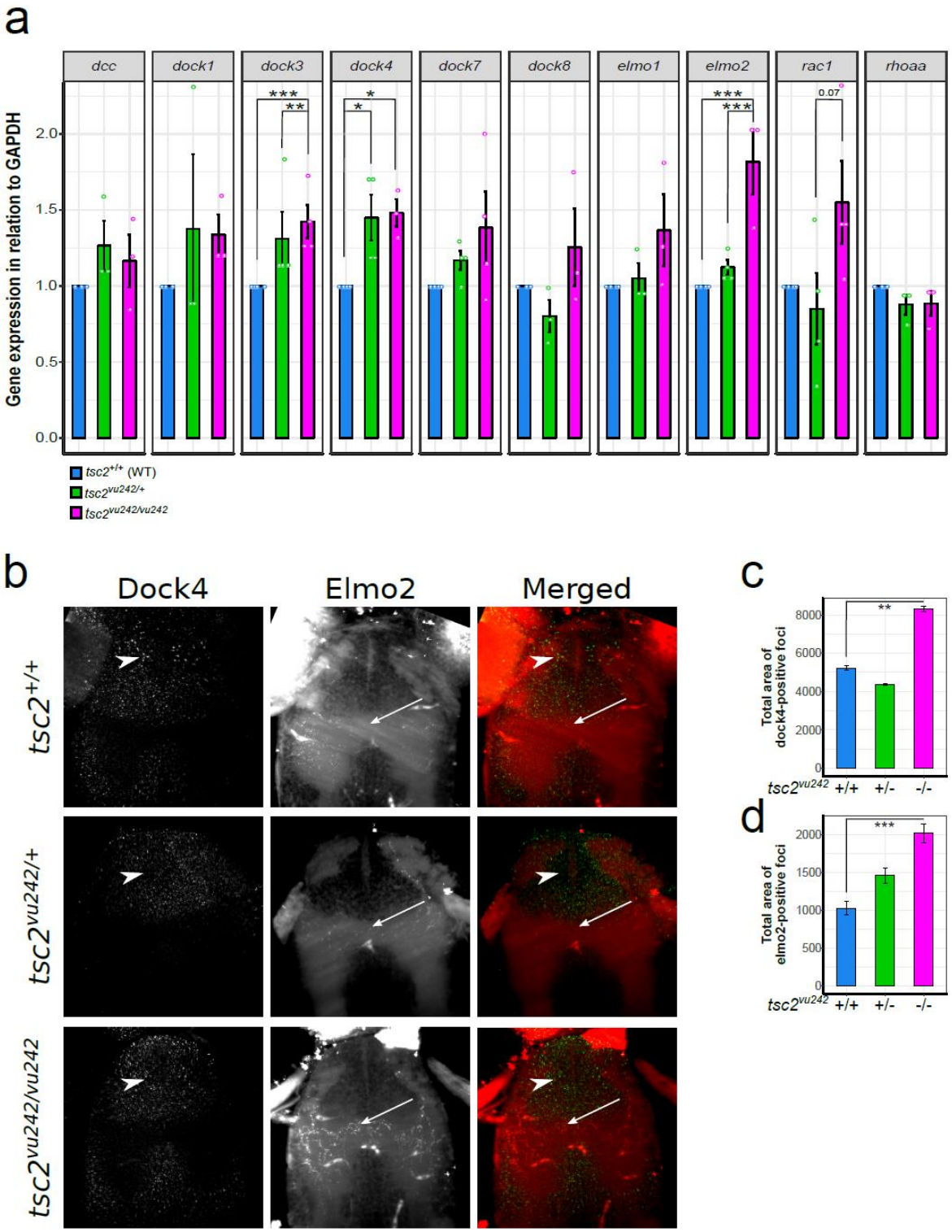

Fig. S4. **a**, Expression analysis of genes that are involved in the Rac1 pathway in response to axon guidance cues by ddPCR: *dock3* ($F = 30.55$, $p = 3.5 \times 10^{-4}$; $p = 1.9 \times 10^{-4}$ for $tsc2^{vu242/vu242}$ *vs.* $tsc2^{+/+}$, $p = 0.007$, for $tsc2^{vu242/vu242}$ *vs.* $tsc2^{vu242/+}$ [Dunnett's test]), *dock4* ($F = 6.863$, $p = 0.018$; $p = 0.024$ for $tsc2^{vu242/vu242}$ *vs.* $tsc2^{+/+}$, $p > 0.05$ for $tsc2^{vu242/vu242}$ *vs.* $tsc2^{vu242/+}$ [Dunnett's test]), *elmo2* ($F = 16.62$, $p = 0.001$; $p = 0.001$ for $tsc2^{vu242/vu242}$ *vs.* $tsc2^{+/+}$, $p = 0.003$ for

tsc2$^{vu242/vu242}$ *vs*. *tsc2*$^{vu242/+}$ [Dunnett's test]), and *rac1* (F = 3.155, p = 0.092; $p > 0.05$ for *tsc2*$^{vu242/vu242}$ *vs*. *tsc2*$^{+/+}$, p = 0.072 for *tsc2*$^{vu242/vu242}$ *vs*. *tsc2*$^{vu242/+}$ [Dunnett's test]). n = 75/genotype. **b**, Representative photomicrographs of dorsally acquired whole mounts of the *tsc2*^{vu242} zebrafish brain that were stained with anti-Dock4 and anti-Elmo2 antibodies. Increased number of Dock4-positive foci in the medial pallium of *tsc2*$^{vu242/vu242}$ mutants *vs*. *tsc2*$^{+/+}$ is indicated by arrowheads, and increased number of Elmo2-positive foci at the anterior commissure of *tsc2*$^{vu242/vu242}$ mutants *vs*. *tsc2*$^{+/+}$ is indicated by arrows. **c**, Quantification of total area covered by Dock4-positive immunofluorescence in *tsc2*^{vu242} zebrafish telencephalons that shows an increase in Dock4 levels (H = 22.043, $p < 1.63 \times 10^{-5}$; $p < 0.004$ for *tsc2*$^{vu242/vu242}$ mutants *vs*. *tsc2*$^{+/+}$ [Dunn's test]). n = 13 *tsc2*$^{+/+}$, 15 *tsc2*$^{vu242/+}$, 19 *tsc2*$^{vu242/vu242}$. **d**, Quantification of total area covered by Elmo2-positive immunofluorescence in *tsc2*^{vu242} zebrafish telencephalons that shows an increase in Elmo2 levels (H = 24.261, $p < 5.39 \times 10^{-6}$; $p < 3.8 \times 10^{-6}$ for *tsc2*$^{vu242/vu242}$ mutants *vs*. *tsc2*$^{+/+}$ and *vs*. *tsc2*$^{vu242/+}$ p = 0.0013 [Dunn's test]). n = 13 *tsc2*$^{+/+}$, 15 *tsc2*$^{vu242/+}$, 19 *tsc2*$^{vu242/vu242}$. $^{*}p < 0.05$, $^{**}p < 0.01$, $^{***}p < 0.005$.

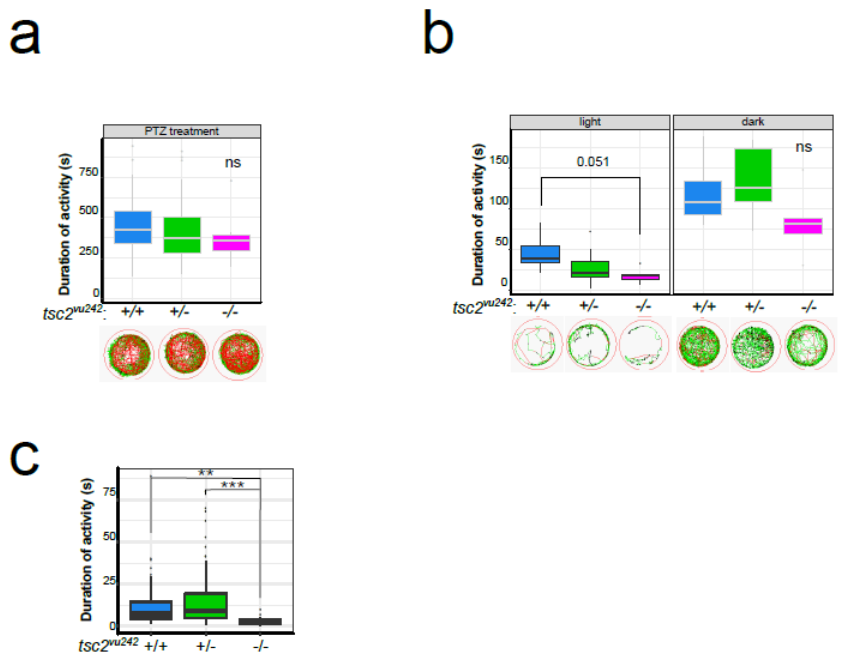

Fig. S5. a, Cumulative activity of *tsc2*$^{vu242/vu242}$ (n = 15), *tsc2*$^{vu242/+}$ (n = 69), and *tsc2*$^{+/+}$ (n = 42) fish over 1 h of tracking after neuromodulation by pentylenetetrazol (PTZ), showing that locomotion in *tsc2*$^{vu242/vu242}$ fish increased after neuromodulation to levels that were similar to *tsc2*$^{+/+}$ fish. Corresponding representative tracks of all three genotypes are shown below the chart. **b**, Cumulative activity in the light condition and after a dark flash per 10-min tracking of *tsc2*$^{vu242/vu242}$ mutant fish (n = 28) compared with *tsc2*$^{vu242/+}$ (n = 74) and *tsc2*$^{+/+}$ (n = 43) fish with corresponding representative tracks below, demonstrating that *tsc2*$^{vu242/vu242}$ fish could see because they altered their activity after the light was suddenly switched off during tracking (dark flash: F = 3.399, p = 0.046; light condition: F = 61.935, $p = 5.6 \times 10^{-9}$; dark flash × light condition interaction: $p > 0.05$; p = 0.051, *tsc2*$^{vu242/vu242}$ *vs.* *tsc2*$^{+/+}$ in light condition [Dunnett's test]; p = 0.278, *tsc2*$^{vu242/vu242}$ *vs.* *tsc2*$^{+/+}$ in dark condition [Dunnett's test]). **c**, Cumulative zebrafish activity in > 2 cm/s range (F = 9.132, $p = 1.7 \times 10^{-4}$; p = 0.005, *tsc2*$^{vu242/vu242}$ *vs.* *tsc2*$^{+/+}$ [Dunnett's multiple-comparison *post hoc* test]; $p = 6.3 \times 10^{-5}$, *tsc2*$^{vu242/vu242}$ *vs.* *tsc2*$^{vu242/+}$ [Dunnett's multiple-comparison *post hoc* test]). Red tracks indicate high-velocity movements (> 2 cm/s). Green tracks indicate free swimming (movement within the range of 0.5-2 cm/s). Black tracks indicate free floating (< 0.5 cm/s). *$p < 0.05$, **$p < 0.01$, ***$p < 0.005$.

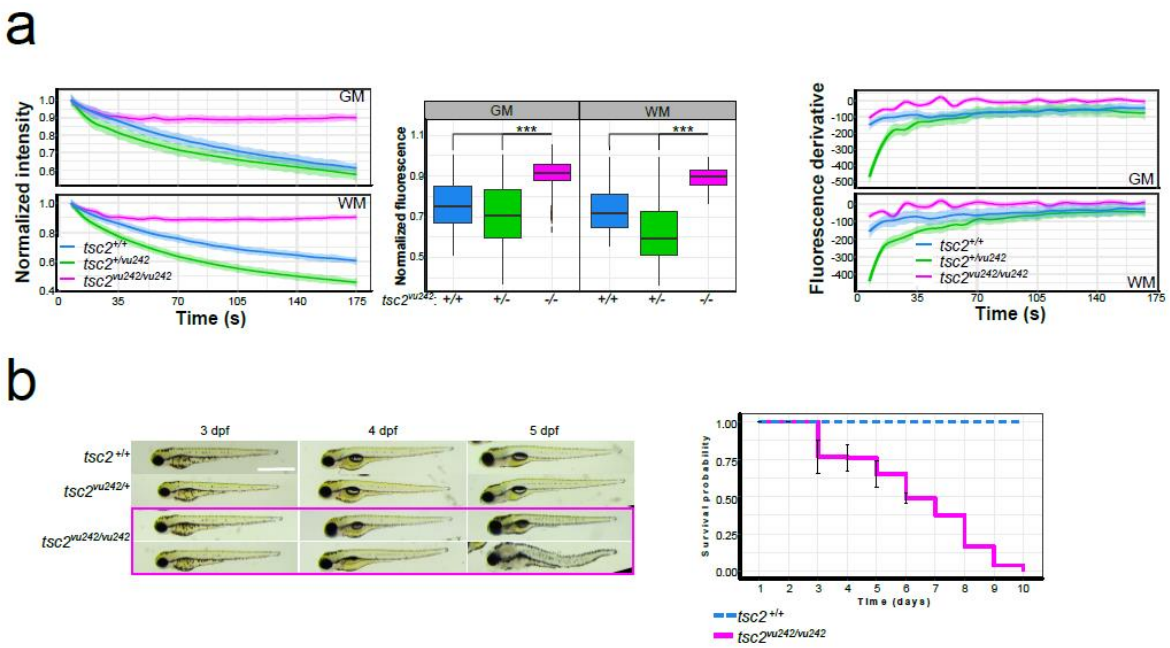

Fig. S6. a, Neuronal activity analysis, including normalized intensity over time, normalized average fluorescence (H = 759.4, $p < 2.2 \times 10^{-16}$; $p < 2 \times 10^{-16}$ for *tsc2*$^{vu242/vu242}$ mutants *vs.* *tsc2*$^{+/+}$ or *tsc2*$^{vu242/+}$ [Dunn's test]), and fluorescence derivative over time for gray matter (GM) and white matter (WM) of the pallium in *tsc2*^{vu242} fish, showing constant mean intensity levels over time and oscillations of GCaMP5G-probe-fluorescence derivative around zero in *tsc2*$^{vu242/vu242}$ fish. **b**, Photomicrographs that show gross-morphology phenotypes of *tsc2*$^{vu242/vu242}$ mutant fish compared with *tsc2*$^{vu242/+}$ fish and *tsc2*$^{+/+}$ control siblings at various time-points of development, together with survival plot (probability over time) for *tsc2*$^{vu242/vu242}$ mutant fish (1-6 dpf, n = 180; 7-10 dpf, n = 35) and *tsc2*$^{+/+}$ control siblings (1-6 dpf, n = 210; 7-10 dpf, n = 35; mean ± SEM). Scale bar = 1 mm. *$p < 0.05$, **$p < 0.01$, ***$p < 0.005$.

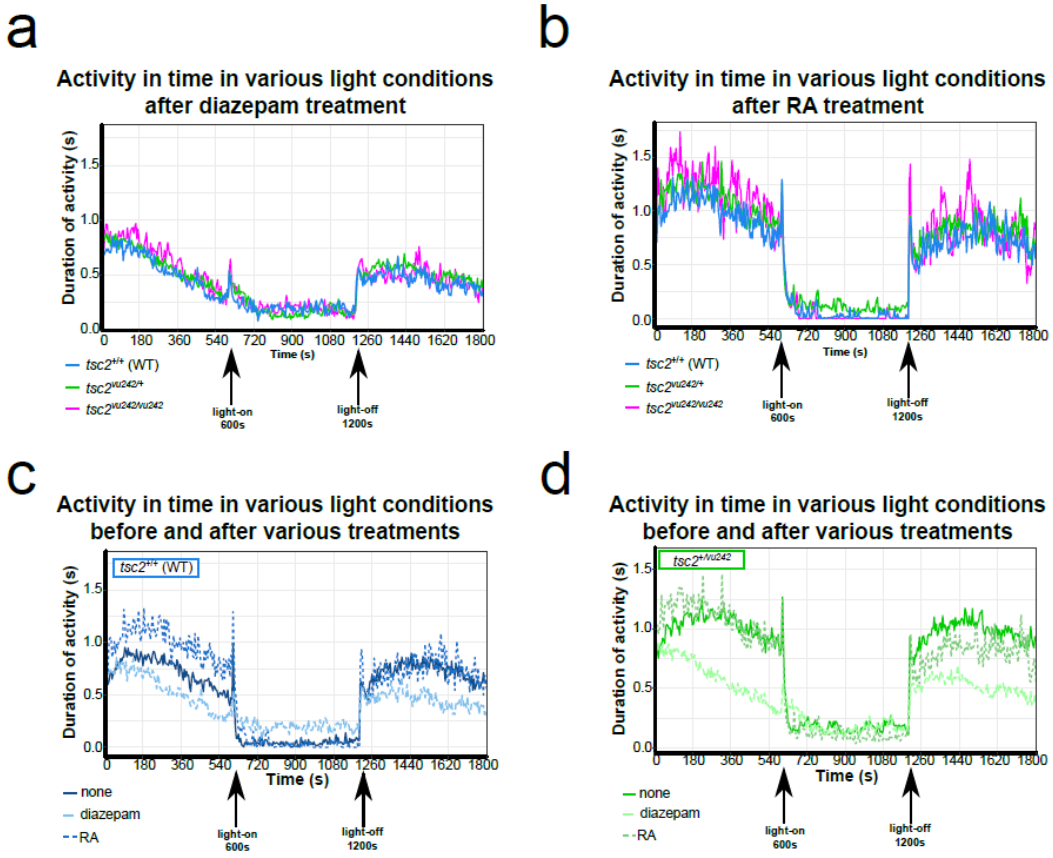

Fig. S7. **a**, Activity over time of *tsc2*^{vu242} zebrafish after sudden light changes for each genotype after treatment with the anxiolytic diazepam (H = 49.925, p = 1.4 × 10^{-11}; p = 5.4 ×10^{-10} for *tsc2*$^{vu242/vu242}$ *vs*. *tsc2*$^{+/+}$ and [Dunn's test]; p = 3.7 × 10^{-9} for *tsc2*$^{vu242/+}$ *vs*. *tsc2*$^{+/+}$ [Dunn's test]). **b**, Activity over time in *tsc2*^{vu242} zebrafish after sudden light changes for each genotype after treatment with the anxiogenic RA (H = 26.613, p = 1.7 × 10^{-6}; p = 0.005 for *tsc2*$^{vu242/vu242}$ *vs*. *tsc2*$^{+/+}$ [Dunn's test]; p = 7.6 × 10^{-7} for *tsc2*$^{vu242/vu242}$ *vs*. *tsc2*$^{vu242/+}$ [Dunn's test]). **c**, Comparison of activity over time after treatment with diazepam or RA for *tsc2*$^{+/+}$ fish. **d**, Comparison of activity over time after various treatments for heterozygous *tsc2*$^{vu242/+}$ fish.

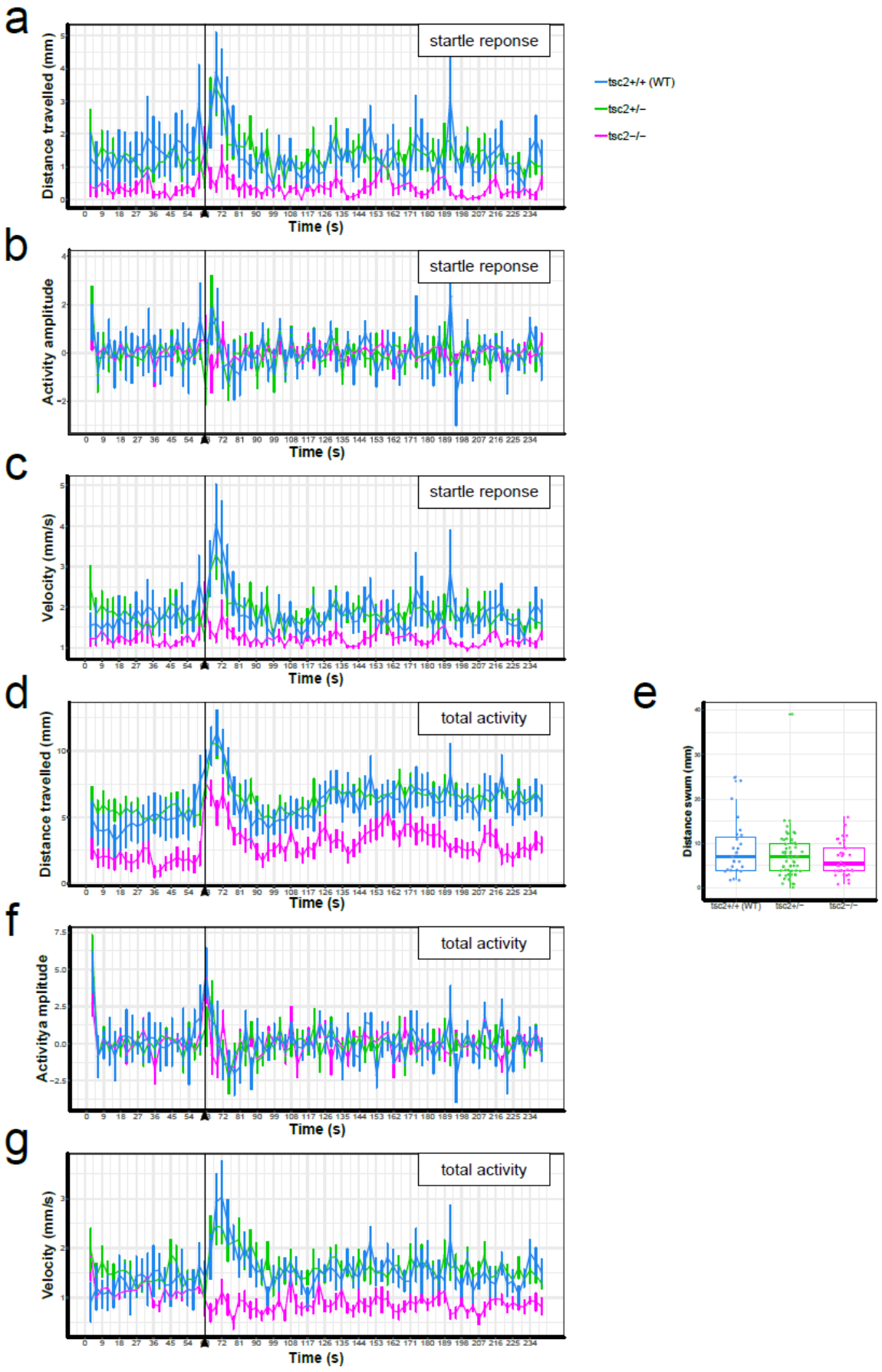
a
startle reponse
Distance travelled (mm)
Time (s)
tsc2+/+ (WT)
tsc2+/−
tsc2−/−
b
startle reponse
Activity amplitude
Time (s)
c
startle reponse
Velocity (mm/s)
Time (s)
d
total activity
Distance travelled (mm)
Time (s)
e
Distance swum (mm)
tsc2+/+ (WT)
tsc2+/−
tsc2−/−
f
total activity
Activitya mplitude
Time (s)
g
total activity
Velocity (mm/s)
Time (s)

Fig. S8. Startle response of *tsc2*^{vu242} zebrafish after sudden dark flash at 63s (black arrow-line) repeating every 3s after this time. The first 60s shows basic locomotor activity without startling stimuli. **a**, Activity over time for startle response in high-velocity range showing slight change in activity after first startling stimulus for *tsc2*$^{vu242/vu242}$ zebrafish compared to sibling controls. **b**, Activity amplitude over time for startle response in high-velocity range showing no peak after first startling stimulus for *tsc2*$^{vu242/vu242}$ zebrafish compared to sibling controls. **c**, Velocity over time for startle response in high-velocity range showing slight change in velocity after first startling stimulus for *tsc2*$^{vu242/vu242}$ zebrafish compared to sibling controls. **d**, Activity over time for the total locomotion showing an increase in activity after first startling stimulus for all genotypes. **e**, Boxplots of the activity in 63rd second showing total activity for each fish across genotypes after first startling stimulus. **f**, Activity amplitude across time for the total locomotion. **g**, Velocity over time for the total locomotion showing no change in total velocity after first startling stimulus for *tsc2*$^{vu242/vu242}$ zebrafish compared to sibling controls.

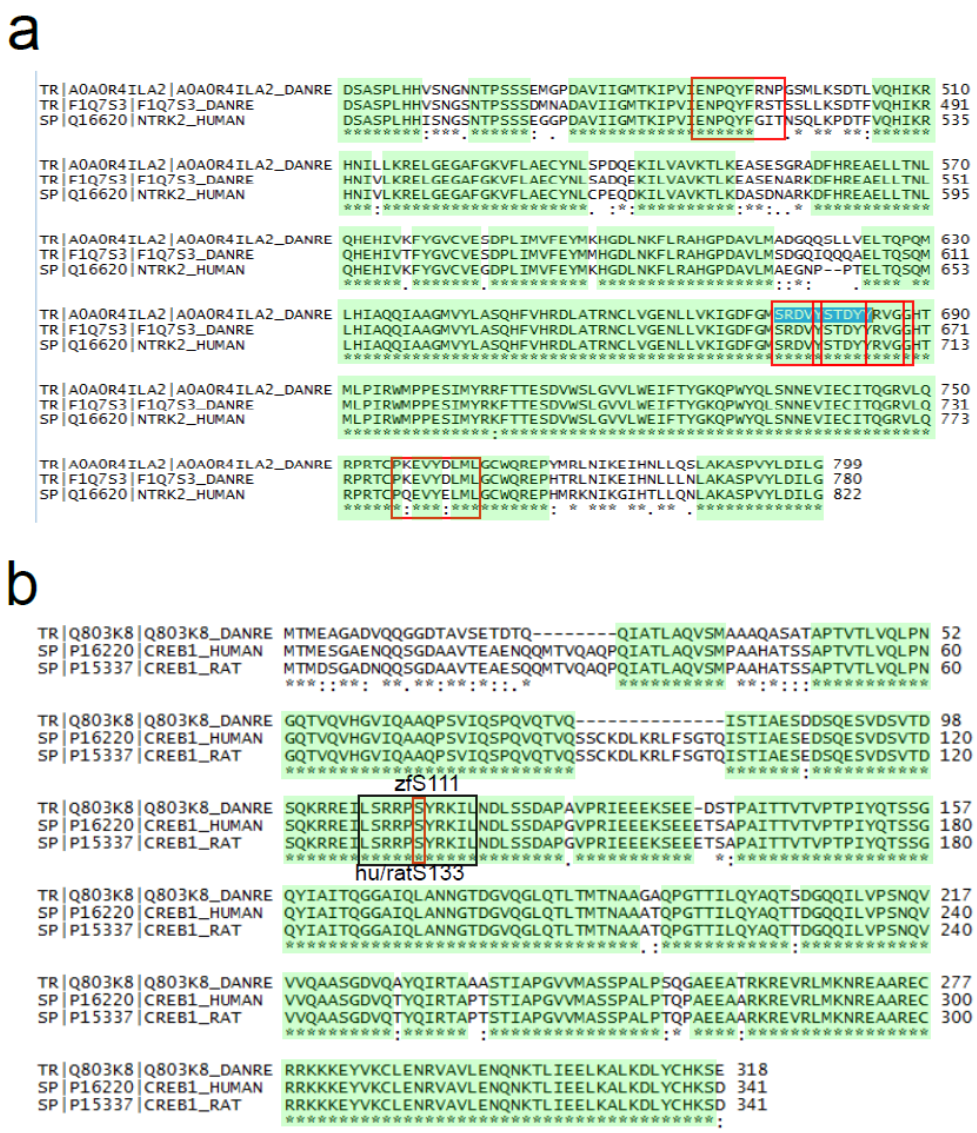

Fig. S9. **a**, Multiple alignment of human, and zebrafish TrkB amino acid sequences showing 100%-identity regions in green and phosphorylation motives framed in red. Zebrafish has two isoforms of TrkB. The TrkB sequence shares over 60% identity between human and fish with highly conserved secondary structure, transmembrane domains, nucleotide binding site, ligand-binding sites, modified residues, and phosphorylation motives. **b**, Multiple alignment of human, rat, and zebrafish Creb amino acid sequences with highly conserved secondary structure, domain, modified residues, and phosphorylation sites, showing 100%-identity regions in green and phosphorylation motif framed in black. The modified serine 133 in human and rat, representing Creb activation, corresponds to serine 111 in zebrafish (red frame). The Creb sequence shares 85.044% identity between human and fish.

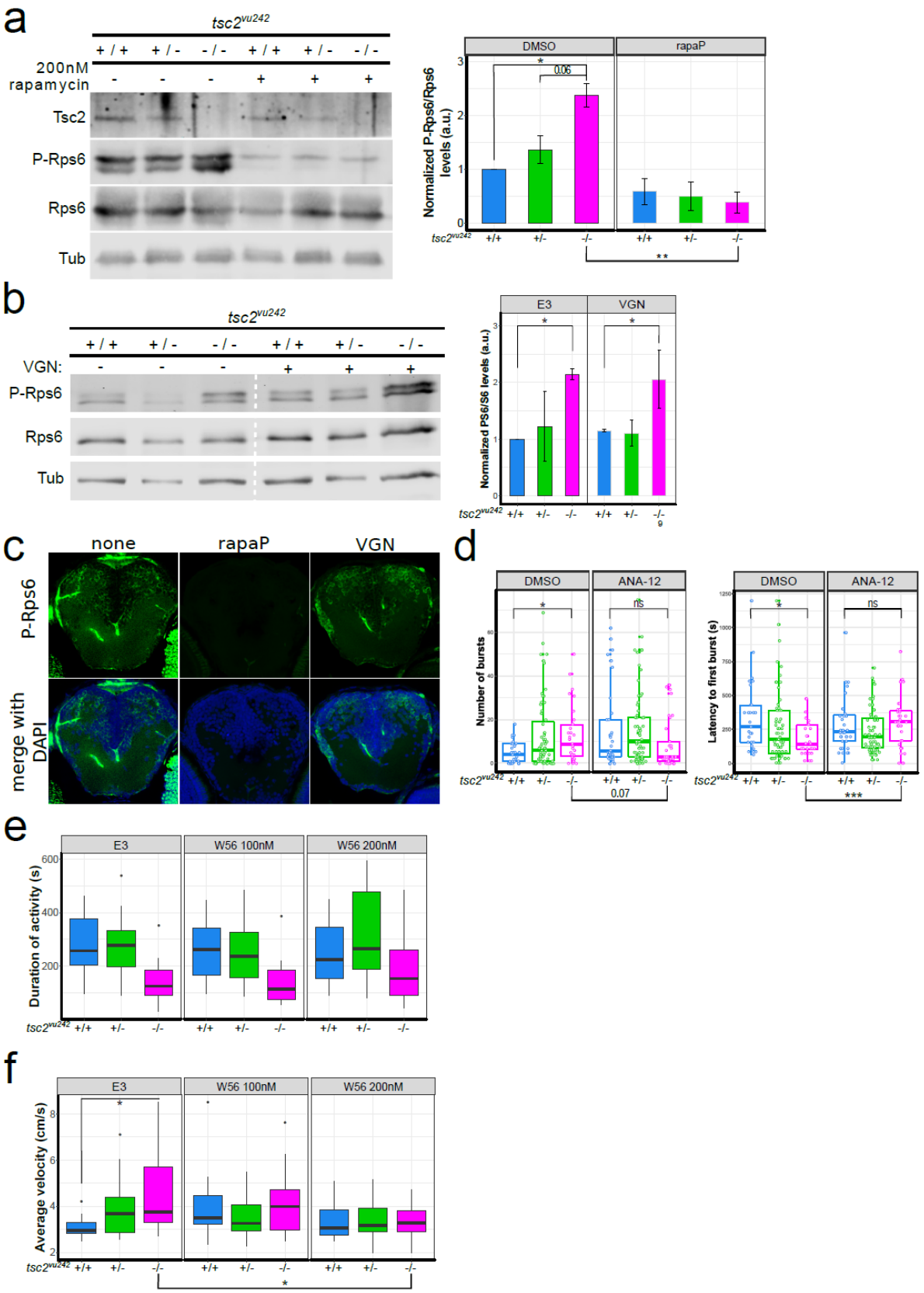
a
tsc2vu242
+ / + + / - - / - + / + + / - - / -
200nM rapamycin
- - - + + +
Tsc2
P-Rps6
Rps6
Tub
DMSO
rapaP
Normalized P-Rps6/Rps6 levels (a.u.)
0.06
tsc2vu242 +/+ +/- -/- +/+ +/- -/-
**
b
tsc2vu242
+ / + + / - - / - + / + + / - - / -
VGN: - - - + + +
P-Rps6
Rps6
Tub
E3
VGN
Normalized PS6/S6 levels (a.u.)
tsc2vu242 +/+ +/- -/- +/+ +/- -/-
c
none
rapaP
VGN
P-Rps6
merge with DAPI
d
DMSO
ANA-12
Number of bursts
ns
0.07
Latency to first burst (s)
***
e
E3
W56 100nM
W56 200nM
Duration of activity (s)
tsc2vu242 +/+ +/- -/- +/+ +/- -/- +/+ +/- -/-
f
E3
W56 100nM
W56 200nM
Average velocity (cm/s)
tsc2vu242 +/+ +/- -/- +/+ +/- -/- +/+ +/- -/-
*

Fig. S10. **a**, Representative immunoblots of Tsc2, P-Rps6, and Rps6 protein levels in *tsc2*^{vu242} zebrafish after pretreatment with rapamycin to prevent disease development (RapaP) and quantification of activation of the mTorC1 pathway, indicated by the ratio of P-Rps6 to Rps6 protein levels in *tsc2*$^{vu242/vu242}$ mutants and *tsc2*$^{vu242/+}$ fish relative to *tsc2*$^{+/+}$ controls (genotype × treatment interaction: $F = 7.079$, $p = 0.014$; $p = 0.016$ for untreated *tsc2*$^{vu242/vu242}$ *vs*. *tsc2*$^{+/+}$ [Tukey HSD test]; $p = 0.063$ for untreated *tsc2*$^{vu242/vu242}$ *vs*. *tsc2*$^{vu242/+}$ [Tukey HSD test]; $p = 0.001$ for untreated *vs*. treated *tsc2*$^{vu242/vu242}$ [Tukey HSD test]; $p = 0.757$ for untreated *vs*. treated *tsc2*$^{+/+}$ [Tukey HSD test]; $n > 30$/genotype/treatment; mean ± SEM). **b**, Representative immunoblots of P-S235/S236-Rps6 and Rps6 protein levels in *tsc2*^{vu242} zebrafish after treatment with VGN and quantification of activation of the mTorC1 pathway, indicated by the ratio of P-Rps6 to Rps6 protein levels in *tsc2*$^{vu242/vu242}$ mutants and *tsc2*$^{vu242/+}$ fish relative to *tsc2*$^{+/+}$ controls (genotype × treatment interaction: $p > 0.05$; genotype: $F = 11.728$, $p = 0.0015$; $p = 0.0385$ for untreated *tsc2*$^{vu242/vu242}$ *vs*. *tsc2*$^{+/+}$ [Tukey HSD test]; $n > 30$/genotype/treatment; mean ± SEM). **c**, Representative confocal photographs of coronal *tsc2*$^{vu242/vu242}$ brain sections through the pallium that were immunostained with anti-P-Rps6 antibody (green), showing no P-Rps6 signal after RapaP and no change in P-Rps6 levels after VGN treatment. **d**, The number of PTZ-induced seizure-like outbursts in the first 10 minutes of tracking ($H = 3.151$, $p = 0.075$; $p = 0.076$ for *tsc2*$^{vu242/vu242}$ control *vs*. ANA-12 treated [Dunn's test]) and the time to first outburst induced by PTZ ($H = 6.808$, $p = 0.0091$; $p = 0.009$ for *tsc2*$^{vu242/vu242}$ control vs. ANA-12 treated [Dunn's test]) for *tsc2*^{vu242} fish treated with DMSO or ANA-12. **e**, Cumulative activity of the *tsc2*$^{vu242/vu242}$ fish after treatment with Rac1 inhibitor W56 compared with *tsc2*$^{vu242/+}$ fish and *tsc2*$^{+/+}$ control siblings over 1 h of tracking, showing no difference in activity of mutant fish after treatment. **f**, Average velocity of high-velocity movements of *tsc2*$^{vu242/vu242}$ fish compared with *tsc2*$^{vu242/+}$ fish and *tsc2*$^{+/+}$ control siblings after treatment with Rac1 inhibitor W56 showing a decrease in high-range velocity after treatment ($H = 9.1416$, $p = 0.01035$; $p = 0.023$ for *tsc2*$^{vu242/vu242}$ untreated *vs*. treated with 200 nM W56 [Dunn's test]). *$p < 0.05$, **$p < 0.01$, ***$p < 0.005$.

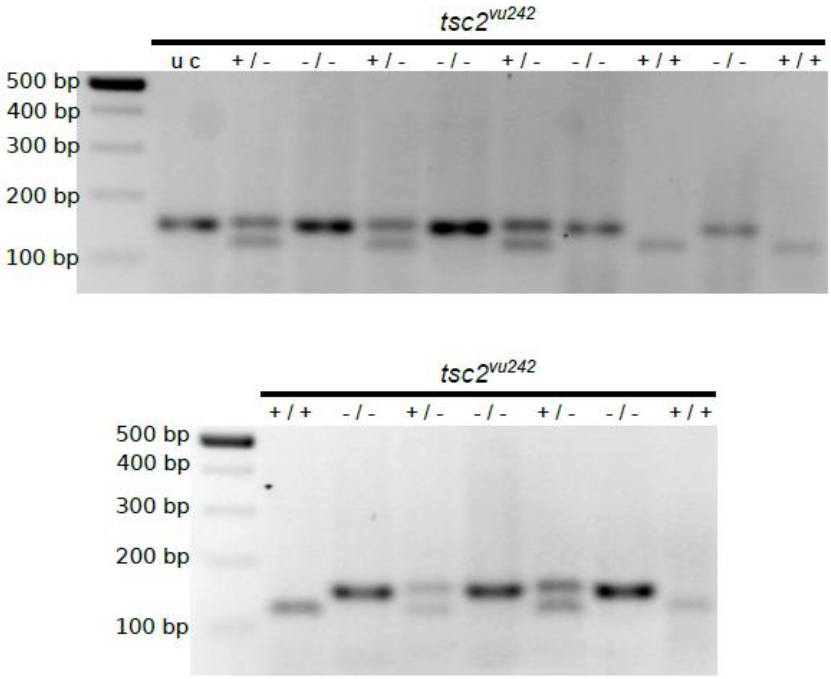

Fig. S11. Representative images of the genotyping results on 2% agarose gels. uc – uncut control, bp – base pairs.

Supplementary Methods

Zebrafish breeding and genotyping

The following zebrafish lines were used: tsc2$^{vu242/+}$ [1], Sofa1 [2], and Tg(HuC:GCaMP5G) [3]. The Tg(ptf1a:GFP) and Tg(ath5:gap-RFP) lines were outcrossed from Sofa1 and then crossed with the tsc2$^{vu242/+}$ line. Adult and larval zebrafish were bred according to international standards. The larvae were genotyped in each experiment (SI Appendix, Fig. S11) as previously described [1]. Offspring of at least two parental pairs were used in each experiment; only naive offspring were included.

Drug treatments

Treatments were for 3 min for PTZ (1.25 mM), 6 min for diazepam (0.35 μM) and RA (2 nM), 24 h before the tests for VGN (60 μM), ethosuximide (25 μM), ANA-12 (50 nM), and W56 (100 nM, 200 nM) or starting from 48 hours postfertilization (hpf) pretreatments with rapamycin (200 nM), and VGN. For the survival experiments, drugs were administered at 24 hpf (pretreatments with rapamycin and VGN) or 48 hpf (VGN, ethosuximide, ANA-12).

Immunofluorescence and ELISA

Heads of 5-dpf larvae were fixed in 4% paraformaldehyde. For sectioning, the tissue was cryoprotected in 30% sucrose. Heads were mounted, frozen, and sectioned in a Leica CM1950 cryostat. Immunofluorescent staining of both whole mounts and cryosections was performed using standard protocols (zfin.org). Samples were permeabilized, blocked with 3% bovine serum albumin, and 10% goat serum, incubated with primary antibodies (anti-acetyl-Lys40-tubulin, 1:100, catalog no. GTX16292, Genetex; anti-P-S235/236-Rps6 antibody, 1:100, catalog no. CS4858, Cell Signaling Technology; anti-GFAP, 1:100, catalog no. Zrf-1,

ZIRC; anti-Dock4, 1:200, catalog no. ab85723, Abcam; anti-Elmo2, 1:100, catalog no. ab2240, Abcam) at room temperature, washed, incubated with secondary antibodies (goat anti-mouse Alexa Fluor 568, 1:1000, Thermo Fisher Scientific; goat anti-rabbit, Alexa Fluor 488, 1:1000, Thermo Fisher Scientific), and mounted. ELISAs for cortisol (catalog no. 1-3002, Salimetrics), P-TrkB (catalog no. DYC688, R&D), and P-Creb (catalog no. DYC2510, R&D) were performed according to the manufacturers' protocols from samples that contained 40 or 10 fish per genotype, respectively, with the exception of minor changes in the P-TrkB ELISA, in which we changed the detection antibody to biotin-conjugated anti-TrkB antibody (500 ng/ml working concentration; catalog no. BAF397, R&D) and streptavidin-horseradish peroxidase (1:200; R&D) to detect TrkB. For the TrkB ELISA, we used a similar protocol as for P-TrkB, with the exception that the capture antibody was anti-TrkB (4 ng/µl working concentration; catalog no. 13129-1-AP, ProteinTech).

Image acquisition

Images of fluorescently labeled cryosections and whole mounts were acquired using a Zeiss LSM800 confocal microscope (40× oil immersion objective, NA = 1.0) at 1024 × 1024 pixel-resolution. Z-stacks of the images were taken with an optimal interval (approximately 0.5 µm) and averaged twice per line. The *in vivo* imaging of axons and neuronal activity in the zebrafish brains was performed using a Zeiss Lighsheet Z.1 microscope (40× oil immersion objective, NA = 1.3). For the imaging of axons, Z-stacks were taken with an optimal interval of 0.48 µm. Initial time-lapses (for wildtype fish) were recorded every 10 min for 3 h at 28.5°C at 24 and 27 hpf (staging was performed for brain ventricle morphology and heart beating, in addition to time). For neuronal activity that was visualized by the GCaMP5, 3D-time-lapse

images of neuronal activity were taken every 7 s for 3 min for the whole pallium, with an approximate range of 300 μm.

Image analyses

Analyses were performed using Fiji software [4]. Regions of interest (ROIs) were drawn manually. Cells in WM were calculated automatically on thresholded images using the Particle Analysis tool. Cell size, fluorescence intensity, and commissural width and volume were measured using the measurement tool. For axon analysis, image segmentation was performed semi automatically, and the arbors were transformed to skeletons using the Skeletonize (2D/3D) plug-in [5]. Both sides of the skeletons were analyzed by the 3D-Sholl analysis [6] plug-in with the soma as the starting point and then averaged per fish. The distance from the soma to the midline with axons that crossed hemispheres was defined at approximately 80 μm using line tool measurements and was used as a cut-off. The linear model was fitted into empirical data using the LOESS regression and smoothing function in RStudio (least squares regression in localized subsets) for data at a distance of 80 μm from the soma or further, representing arbors at the midline of the brain. For neuronal activity, first-drift correction was performed using the Tischer script, and then the fluorescence intensity and derivative were calculated using the measurement tool in Fiji and Rstudio in a semiautomated manner. The linear model was fitted into empirical data as above using RStudio. For the STFBC experiments, the number of flicks and coils were manually calculated from the obtained videos.

Behavioral analyses

Before the measurements, 5-day-post-fertilization (dpf) larvae were acclimated into the behavioral room for 5 min. The basal locomotor activity test and dark flash were performed in 24-well plates after overnight habituation of the larvae. Experiments were performed in a total volume of 0.5 ml. The recordings were taken in the dark for 1 h, with a 600 s data integration period for basal locomotor activity, and for 20 min, with a 10 min data integration period and a final light power of 30% during the light phase (bottom source of light) for the dark flash. The experimental setup included equal 10 min light and then dark periods.

The light preference analysis was performed as described previously [7]. Briefly, the chamber consisted of a single Petri dish, half of which was covered with two photographic filters (ND4 and ND8, Cokin.com), which gives 100% dark using the upper light source with the 25% power. Single larvae were loaded into the uncovered half of the plate that was filled with 30 ml of E3 medium. Recordings were taken for 8 min, with a 5 s data integration period.

For novel environment exploration, single larvae were loaded into the plate that was filled with 30 ml of E3 medium. Recordings were taken for 8 min, with a 5 s integration period.

The hyperactivity and freezing tests were performed in 24-well plates, without habituation. Recordings were taken for 30 min, with a 5 s integration period with the bottom light source. The experimental setup included equal 10 min dark (D) and light (L) periods: D-L-D, with the final power 60% during the light phase.

Pentylenetetrazol-induced seizure-like behavior was evaluated in 24-well plates. Pentylenetetrazol was added directly to the well for 2-3 min before the experiment and during the experiment. Recordings were taken for 20 min, with a 5 s integration period. The experimental setup included equal 10 min light and then dark periods, with the final power set to 60% during the light phase.

Startle response test was performed in 24-well plates after at least 2 hour habituation to the testing room. Recordings were taken for 10 min, with a 3 s integration period. First basic locomotion was assessed for 5 min and then startle experiment with flashing light every 3 s was performed for another 5 min, as previously described [8].

RNA extraction, cDNA synthesis, and Droplet Digital PCR (ddPCR)

Heads of 5 dpf larvae were stored in StayRNA buffer (038-250, A&A Biotechnology) while genotyping was performed, and then total RNA was extracted from 15 or 30 heads per genotype with TRIzol reagent as previously described [9]. cDNA synthesis was performed with the RevertAid H Minus First Strand cDNA Synthesis Kit (Thermo Fisher) according to the manufacturer's protocol. The reaction conditions for quantitative ddPCR and the thermal cycling conditions were set up according to the manufacturer's protocol for EvaGreen Supermix (Bio-Rad). The data analysis was performed using QuantaSoft Analysis Pro software (Bio-Rad) and RStudio. The following primers that spanned exon-exon junctions were used: *dcc* (forward, 5'-GTTTCTCCGACCTCAATCCA; reverse, 5'-CAGTCCCTCCATCCTGTAGC), *dock1* (forward, 5'-CCAAGATGGACTACGGGAAC; reverse, 5'-GATGCGAGCTTCAATCTGCT), *dock3* (forward, 5'-GCAGAGTTTGTGAGGGGAAC; reverse, 5'-TGTGGTGGAGAACAACAGGA), *dock4* (forward, 5'-AATCCATCCACCTGTTCCTG; reverse, 5'-ACATTCGCCACCTCTCTCAT), *dock6* (forward, 5'-GCCTGGACTGCAATTCATTT; reverse, 5'-TGCACATGTCCTCTCCTACACT), *dock7* (forward, 5'-GTTGGGCACAGCATTTAACC; reverse, 5'-TCAATTGACATGGACCTTCG), *dock8* (forward, 5'-GCCTTTGCTACGGTCAACAT; reverse, 5'-TTGTCCTCCATCAAGCTGAA), *elmo1* (forward, 5'-GCCCACCAGCTCTATGTTCT; reverse, 5'-

TTGGACTCGCATTCAACATC), *elmo2* (forward, 5'-TGCAGGTGCTGACCTTTAAC; reverse, 5'-GCTTTCCTCTTCTCGGTTCC), *rac1* (forward, 5'-CATCCTGGTGGGAACTAAGC; reverse, 5'-AGTGCCGAGCATTCCAGATA), *gapdh* (forward, 5'-GTGGAGTCTACTGGTGTCTTC; reverse, 5'-GTGCAGGAGGCATTGCTTACA).

Western blot

Protein extraction and immunoblotting were performed according to a standard protocol (zfin.org). Briefly, fresh, cold Ringer buffer (supplemented with ethylenediaminetetraacetic acid and phosphatase and protease inhibitors) was applied for washing and storing. Sodium dodecyl sulfate (SDS) sample buffer was used for protein extraction from at least 10 heads per genotype. Equivalents of 4 larvae/lane were loaded on 10% polyacrylamide gel, run by SDS-polyacrylamide gel electrophoresis, and transferred to nitrocellulose membranes. The following antibodies were used: anti-P-S235/236-Rps6 (1:1000, catalog no. CS4858, Cell Signaling Technology), anti-Rps6 (1:250, catalog no. sc-74459, Santa Cruz Biotechnology), anti-Tubulin (1:2000, catalog no. T516B, Sigma-Aldrich), anti-Tsc2 (1:500, catalog no. CS4308, Cell Signaling Technology), donkey IRDye 800CW anti-mouse IgG (catalog no. 926-32212, Li-Cor Biotechnology), and donkey IRDye 680RD anti-rabbit IgG (catalog no. 926-68073, Li-Cor Biotechnology). Membranes were analyzed using the Odyssey Imaging System (Li-Cor Biotechnology).

Statistical analyses and experimental design

No predetermination of sample sizes was performed because the number of each genotype could not be predicted due to the random distribution and early lethality of

homozygotes. The data were plotted to verify normality. When sample sizes were too small, the data were assumed to have a normal distribution. The equality of variance was tested by Levene's statistic. The normally distributed data with equal variance were further analyzed using one-way or two-way analysis of variance (ANOVA), depending on the number of factors; otherwise, the Kruskal-Wallis test was employed. Pre-specified *post hoc* comparisons were performed to analyze differences within and between factors after multiple-comparison adjustments using Dunnett's test, the Tukey Honestly Significant Difference (TukeyHSD) test, or Dunn's test, respectively. The adjusted $p<0.05$ was considered statistically significant and the following statistical significance was marked in figures: $*p<0.05$, $**p<0.01$, $***p<0.005$. All the analyses were performed using RStudio. Data are presented as medians with Q1 and Q3 quartiles using boxplots, unless otherwise stated. Open dots represent data points. Filled dots represent data outliers. In most cases, randomization was assured by a lack of knowledge about the genotypes while performing the experiments and the automatic or semi-automatic analyses.

Supplementary References

1. Kim S-H, Speirs CK, Solnica-Krezel L, Ess KC (2011) Zebrafish model of tuberous sclerosis complex reveals cell-autonomous and non-cell-autonomous functions of mutant tuberin. Dis Model Mech 4:255–267
2. Almeida AD, Boije H, Chow RW, He J, Tham J, Suzuki SC, Harris WA (2014) Spectrum of Fates: a new approach to the study of the developing zebrafish retina. Development. https://doi.org/10.1242/dev.104760
3. Ahrens MB, Orger MB, Robson DN, Li JM, Keller PJ (2013) Whole-brain functional imaging at cellular resolution using light-sheet microscopy. Nat Methods 10:413–420

4. Schindelin J, Arganda-Carreras I, Frise E, et al (2012) Fiji: an open-source platform for biological-image analysis. Nat Methods. https://doi.org/10.1038/nmeth.2019
5. Lee TC, Kashyap RL, Chu CN (2002) Building Skeleton Models via 3-D Medial Surface Axis Thinning Algorithms. CVGIP Graph Model Image Process 56:462–478
6. Ferreira TA, Blackman A V, Oyrer J, Jayabal S, Chung AJ, Watt AJ, Sjöström PJ, van Meyel DJ (2014) Neuronal morphometry directly from bitmap images. Nat Methods. https://doi.org/10.1038/nmeth.3125
7. Steenbergen PJ, Richardson MK, Champagne DL (2012) The Light–Dark Preference Test for Larval Zebrafish. pp 21–35
8. Norton WHJ (2012) Measuring Larval Zebrafish Behavior: Locomotion, Thigmotaxis, and Startle. https://doi.org/10.1007/978-1-61779-597-8_1
9. Peterson SM, Freeman JL (2009) RNA Isolation from Embryonic Zebrafish and cDNA Synthesis for Gene Expression Analysis. J Vis Exp. https://doi.org/10.3791/1470